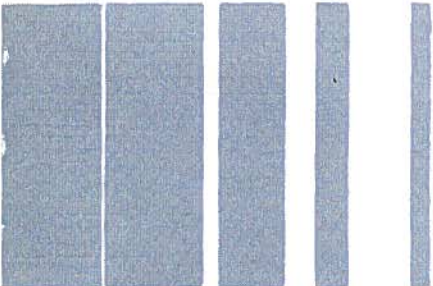
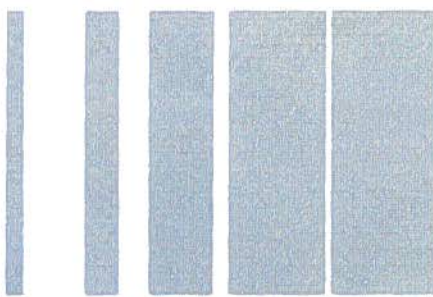


A handwritten signature in dark ink, possibly reading "R. K. M.", with a long horizontal line extending from the end of the signature.

Volume 1, Number 1
January 1986

A series of five vertical bars of varying heights and widths, arranged in a descending staircase pattern from left to right.

JOURNAL OF WAVE- MATERIAL INTERACTION

A series of five vertical bars of varying heights and widths, arranged in an ascending staircase pattern from left to right.

ISSN 0887-0586



SH-WAVE REFLECTION AND TRANSMISSION CHARACTERISTICS OF AN INFINITE, PARALLEL, PERIODIC ARRAY OF TRANSVERSELY ISOTROPIC, PIEZOELECTRIC CYLINDERS

AKHLESH LAKHTAKIA, VIJAY K. VARADAN and
VASUNDARA V. VARADAN

*Laboratory for Electromagnetic and Acoustic Research
Department of Engineering Science and Mechanics
The Pennsylvania State University
University Park, PA 16802.*

ABSTRACT

The SH- wave reflection and the transmission characteristics of a two-dimensional, parallel, periodic array of transversely isotropic, piezoelectric, circular cylinders immersed in a material medium are examined. Use is made of the Floquet theorem to break up the scattering geometry into an infinite number of unit cells as well as to devise a plane wave spectral representation of both the elastic and the electromagnetic fields. The scattering characteristics of each cylinder are obtained by a separation of variables approach. Fourier-Bessel expansions are then used in a mode-matching technique to solve for the scattering characteristics. A quasi-static approximation is also derived and is used to compute the diffracted power coefficients. It is observed that the voltage developed across a diameter of the cylinder in a unit cell accurately reflects the Rayleigh-Wood anomalies.

INTRODUCTION

Ever since the discovery of the piezoelectric effect by Pierre and Jacques Curie [1,2], materials possessing the relevant properties have been used in the manufacture of diverse transducers, resonators, filters and other such-like applications. Piezoelectricity is the linear, reversible coupling between electromagnetic and mechanical (elastic) energies due to the displacement of charges. Charge applied over the surfaces of such a material produces internal stress and strain; conversely, the application of mechanical pressure creates a change in the surface charge density, thereby launching an electromagnetic field.

Materials that are piezoelectric are either crystals with anisotropic properties, or, they are ceramics with ferroelectric properties which can be endowed with a permanent charge polarization through dielectric hysteresis. Single crystals are generally suited for very high frequencies and, in quartz, elastic wave propagation has been observed even at 125 GHz. However, the piezoelectric coupling in quartz is quite weak. Synthetic materials, principally ferroelectric ceramics like *uniaxial* barium titanate (BaTiO_3) and lead zirconate titanate (PZT), on the other hand, have stronger piezoelectric coupling and possess polycrystalline grain structures which propagate elastic waves with moderate attenuation at frequencies upto the low-megahertz range.

Although the use of piezoelectric materials is quite widespread, the scattering and the absorption properties of material volumes made of such media have not been extensively investigated. Reflection and transmission characteristics of planar, piezoelectric half-spaces was examined by Kyame [3,4]. Scattering of elastic and electromagnetic (EM) waves by some piezoelectric, cylindrical inclusions has been explored by Moon [Ref. 5, and others *loc. cit.*]. But because of the complicated anisotropic nature of such materials, whose taxonomy runs over no less than 11 systems [2], a general theory for scattering by piezoelectric material volumes has been lacking.

The aim of the present work, however, is not to present such a general theory (a formidable task, if not actually impossible). Instead, a specific problem, not treated in the extant literature, is going to be investigated here. The scattering geometry consists of a periodic array of identical, piezoelectric, circular cylinders of infinite lengths which are immersed in a non-piezoelectric medium. The piezoelectric materials considered here have hexagonal symmetry and are transversely isotropic, and, furthermore, have the same form of constitutive properties as *uniaxial* BaTiO₃. For the properties of such a class of materials, the reader is referred to the works of Auld [2] and Moon [5]. Although the incident wave can either be an SH-type elastic wave or a TM-polarized electromagnetic wave, numerical results will be given only for the former incidence case. Use is made of the Fourier-Bessel expansions and the plane wave spectral (PWS) representation of the relevant fields and a mode-matching theory [6] is utilized to compute the plane wave reflection and the transmission coefficients of such an array.

PRELIMINARIES

Consider the scattering geometry shown in Fig. 1 where the homogeneous medium 1 extends over all space, except for the parallel, periodic array of circular cylinders made of material 2. Medium 1 has been chosen to be isotropic and homogeneous; it can support both electromagnetic and elastic waves independent of each other, and is devoid of any piezoelectric coupling. On the other hand, the cylinders possess piezoelectric properties and are transversely isotropic in the *xy* plane. Piezoelectric materials of this kind are quite common, e.g., *uniaxial* BaTiO₃, cadmium sulfide (CdS) and zinc oxide (ZnO) [5]. Such materials, being piezoelectric, are necessarily anisotropic, but that anisotropy manifests itself in wave propagation in the *xz* (or, the *yz*) plane. Since the present problem is two-dimensional and wave propagation occurs in the *xy* plane, transverse isotropy aids in the formulation of a comparatively simpler solution. Furthermore, the following treatment applies strictly to materials like *uniaxial* BaTiO₃; for other classes of piezoelectric media with transverse isotropy and hexagonal symmetry, modifications must be made in the coefficients C_m , D_m , E_m , etc. which appear later on.

The permeability and the permittivity of medium 1 are denoted by ϵ_1 and μ_1 , respectively, while its density and rigidity are denoted by ρ_1 and c_{441} , respectively. Electromagnetic waves polarized TM-to-*z* alone are coupled to the SH-type elastic waves in this problem; hence, the other material properties of medium 1 are not of consequence here. The corresponding properties of the piezoelectric medium 2 are denoted by ϵ_{T2} (ϵ_2 is a tensor and ϵ_{T2} is its *xx* component measured at constant traction), μ_2 , ρ_2 and c_{442} , whereas e_{152} is its needed piezoelectric coupling constant [2,5].

It turns out, therefore, that in medium 1, the EM plane waves can be of the form

$$\mathbf{H} \propto \exp [i\mathbf{k}_{H1} \cdot \mathbf{r}] z; \quad \nabla \times \mathbf{H} = -i\omega\epsilon_1 \mathbf{E}, \quad (1a)$$

with the EM wavenumber

$$k_{H1} = \omega [\epsilon_1 \mu_1]^{-1/2}, \quad (1b)$$

whereas the elastic displacement vector \mathbf{u} of the plane SH-waves is of the form

$$\mathbf{u} \propto \exp [i\mathbf{k}_{SH1} \cdot \mathbf{r}] z, \quad (2a)$$

with the SH wavenumber

$$k_{SH1} = \omega [\rho_1 / c_{441}]^{-1/2}. \quad (2b)$$

When a SH wave or a TM-polarized EM wave impinges on the cylinders, the piezoelectricity of medium 2 gives rise to scattered fields of both kinds. Thus, whereas the elastic and the EM waves are decoupled in medium 1, the two fields induced inside each cylinder are coupled together by the coupling factor e_{152} . In medium 2, a pure TM-polarized EM field possessing a wavenumber

$$k_{H2} = \omega [\epsilon_{T2}\mu_2]^{-1/2} \quad (3a)$$

can exist, along with a *piezoelectrically stiffened* SH wave having a wavenumber

$$k_{SH2} = \omega [\rho_2 / \{c_{442} + (e_{152})^2 / \epsilon_{T2}\}]^{-1/2}. \quad (3b)$$

It may be noted that in (3b) the rigidity is not c_{442} , it being augmented by the addition of $(e_{152})^2 / \epsilon_{T2}$. Insofar as the actual representation of the various field components in the cylinders are concerned, they will not be given here and the interested reader is referred to Moon [5].

Finally, it should be noted here that L is the period between consecutive cylinders along the x axis and a is their radius of cross-section. Because of the periodicity of the problem, the celebrated Floquet theorem [7] can be used to break down the scattering geometry into an infinite number of unit cells, also illustrated in Fig. 1. Then, the scattering by any one of these unit cells can be considered separately with periodic boundary conditions being imposed on each cell. To accomplish this purpose, one needs, however, the scattering response of a sole piezoelectric cylinder embedded in medium 1.

SCATTERING OF WAVES BY A PIEZOELECTRIC CYLINDER

As is customary in two-dimensional problems involving cylindrical geometries, all relevant fields are expanded in terms of cylindrical Bessel functions $J_m(\cdot)$ or cylindrical Hankel functions of the first kind $H_m(\cdot)$, concurrent with a harmonic time dependence $\exp[-i\omega t]$. Thus, if a SH wave

$$u_z^0 = \sum_m A_m J_m(k_{SH1}r) r^{-m} (x+iy)^m, m \in \{-\infty, \infty\} \quad (4)$$

is incident on a piezoelectric cylinder of radius a , then the total field existing outside the cylinder can be expressed in the form [5]:

$$u_z^{\text{unit}} = \sum_m A_m \{J_m(k_{SH1}r) + C_m H_m(k_{SH1}r)\} r^{-m} (x+iy)^m, m \in \{-\infty, \infty\}, r \geq a \quad (5a)$$

and

$$H_z^{\text{unit}} = \sum_m A_m \{D_m H_m(k_{H1}r)\} r^{-m} (x+iy)^m, m \in \{-\infty, \infty\}, r \geq a \quad (5b)$$

where,

$$r = (x^2 + y^2)^{1/2}, \quad (6)$$

$$\begin{aligned} -\Delta_m C_m &= \{(me_{152})^2 / \epsilon_{T2}\} J_m(k_{SH1}a) J_m(k_{SH2}a) H_m(k_{H1}a) J_m(k_{H2}a) \\ &\quad - [H_m(k_{H1}a) J_m'(k_{H2}a) - \eta_{12} H_m'(k_{H1}a) J_m(k_{H2}a)] \cdot \\ &\quad \cdot [J_m(k_{SH1}a) J_m'(k_{SH2}a) - \gamma_{12} J_m'(k_{SH1}a) J_m(k_{SH2}a)] \cdot \\ &\quad \cdot [k_{H2} k_{SH2} a^2] \cdot [c_{442} + e_{152}^2 / \epsilon_{T2}], \end{aligned} \quad (7a)$$

$$\Delta_m D_m = [2me_{152} / \pi] J_m(k_{SH2}a) J_m(k_{H2}a), \quad (7b)$$

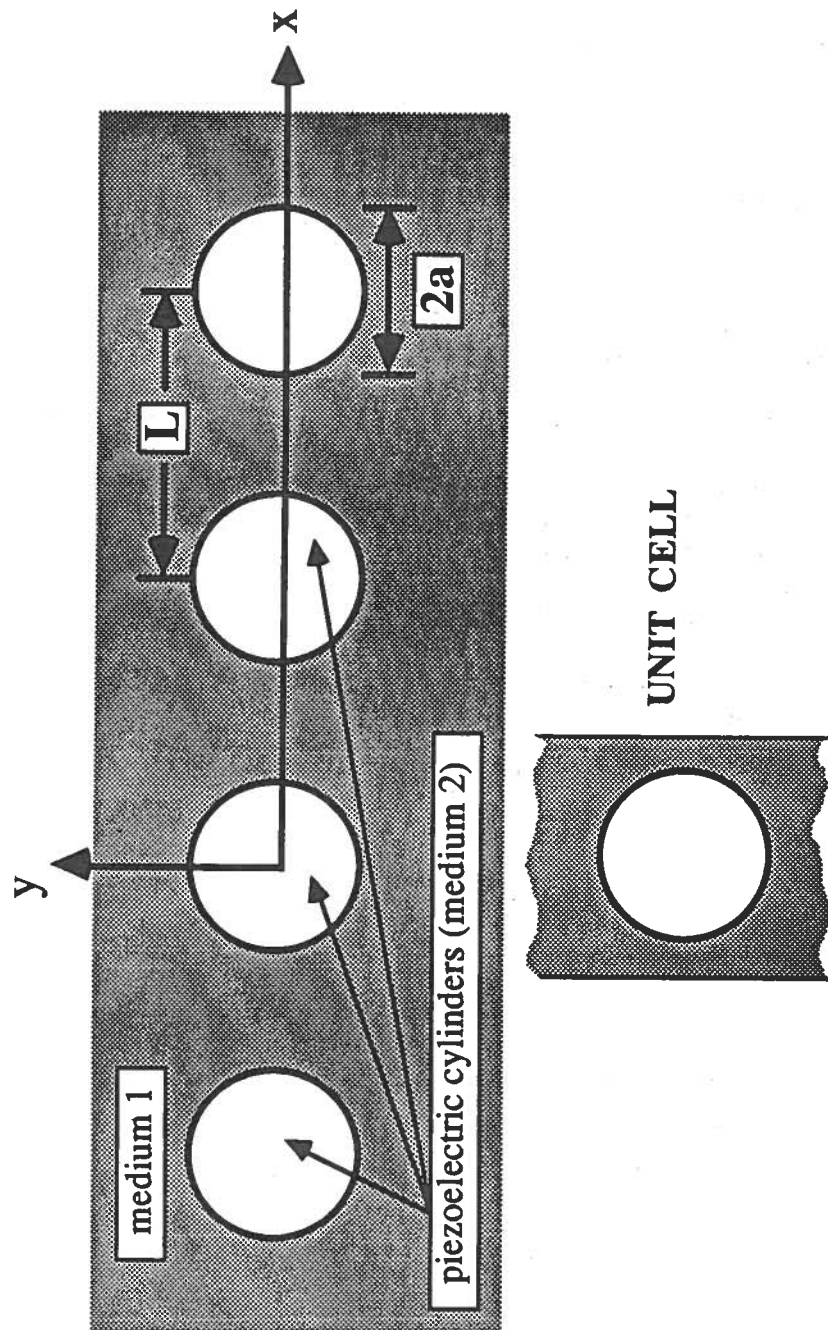


Figure 1. Schematic of the problem.

$$\begin{aligned} \Delta_m &= \{(me_{152})^2/\epsilon_{T2}\} H_m(k_{SH1}a) J_m(k_{SH2}a) H_m(k_{H1}a) J_m(k_{H2}a) \\ &\quad - [H_m(k_{H1}a) J_m'(k_{H2}a) - \eta_{12} H_m'(k_{H1}a) J_m(k_{H2}a)] \cdot \\ &\quad \cdot [H_m(k_{SH1}a) J_m'(k_{SH2}a) - \gamma_{12} H_m'(k_{SH1}a) J_m(k_{SH2}a)] \cdot \\ &\quad \cdot [k_{H2}k_{SH2}a^2] \cdot [c_{442} + e_{152}^2/\epsilon_{T2}], \end{aligned} \quad (7c)$$

$$\eta_{12} = (\mu_1/\mu_2)^{1/2} (\epsilon_{T2}/\epsilon_1)^{1/2}, \quad (7d)$$

$$\gamma_{12} = (\rho_1/\rho_2)^{1/2} (c_{442}/c_{441} + e_{152}^2/c_{441}\epsilon_{T2})^{-1/2}, \quad (7e)$$

and the primes denote differentiation with respect to the argument.

If, on the other hand, a TM-polarized EM wave

$$H_z^0 = -i\omega \sum_{m=-\infty}^{\infty} B_m J_m(k_{H1}r) r^{-m} (x+iy)^m, \quad m \in \{-\infty, \infty\} \quad (8)$$

is incident on the cylinder, then the total field existing outside it can be set down as [5]:

$$H_z^{\text{unit}} = -i\omega \sum_{m=-\infty}^{\infty} B_m \{J_m(k_{H1}r) + E_m H_m(k_{H1}r)\} r^{-m} (x+iy)^m, \quad m \in \{-\infty, \infty\}, r \geq a, \quad (9a)$$

and

$$u_z^{\text{unit}} = \sum_{m=-\infty}^{\infty} B_m \{F_m H_m(k_{SH1}r)\} r^{-m} (x+iy)^m, \quad m \in \{-\infty, \infty\}, r \geq a, \quad (9b)$$

where

$$\begin{aligned} -\Delta_m E_m &= \{(me_{152})^2/\epsilon_{T2}\} H_m(k_{SH1}a) J_m(k_{SH2}a) J_m(k_{H1}a) J_m(k_{H2}a) \\ &\quad - [J_m(k_{H1}a) J_m'(k_{H2}a) - \eta_{12} J_m'(k_{H1}a) J_m(k_{H2}a)] \cdot \\ &\quad \cdot [H_m(k_{SH1}a) J_m'(k_{SH2}a) - \gamma_{12} H_m'(k_{SH1}a) J_m(k_{SH2}a)] \cdot \\ &\quad \cdot [k_{H2}k_{SH2}a^2] \cdot [c_{442} + e_{152}^2/\epsilon_{T2}], \end{aligned} \quad (10a)$$

and

$$\Delta_m F_m = -[2me_{152}/\pi\epsilon_1] J_m(k_{SH2}a) J_m(k_{H2}a). \quad (10b)$$

Therefore, the complete general expression of the total fields existing outside the piezoelectric cylinder must be of the form:

$$u_z^{\text{unit}} = \sum_m r^{-m} (x+iy)^m [B_m F_m H_m(k_{SH1}r) + A_m \{J_m(k_{SH1}r) + C_m H_m(k_{SH1}r)\}], \quad m \in \{-\infty, \infty\}, r \geq a, \quad (11)$$

and

$$H_z^{\text{unit}} = -i\omega \sum_m r^{-m} (x+iy)^m [A_m D_m H_m(k_{H1}r) + B_m \{J_m(k_{H1}r) + E_m H_m(k_{H1}r)\}], \quad m \in \{-\infty, \infty\}, r \geq a, \quad (12)$$

with A_m and B_m representing the yet unknown coefficients of the incident SH and TM waves. As would be seen in the next section, it would be advantageous to recast these two expressions into an equivalent form:

$$u_z^{\text{unit}} = \sum_m \cos(m\phi) [A_{1m} \{J_m(k_{SH1}r) + C_m H_m(k_{SH1}r)\} + A_{2m} F_m H_m(k_{SH1}r)] + i \sum_m \sin(m\phi) [A_{3m} \{J_m(k_{SH1}r) + C_m H_m(k_{SH1}r)\} + A_{4m} F_m H_m(k_{SH1}r)], \quad r \geq a, \quad (13)$$

and

$$(i/\omega)H_z^{\text{unit}} = i \sum_m \sin(m\phi) [A_{2m} \{J_m(k_{H1}r) + E_m H_m(k_{H1}r)\} + A_{1m} D_m H_m(k_{H1}r)] + \sum_m \cos(m\phi) [A_{4m} \{J_m(k_{H1}r) + E_m H_m(k_{H1}r)\} + A_{3m} D_m H_m(k_{H1}r)], \quad r \geq a, \quad (14)$$

with $\phi = \tan^{-1}(y/x)$, and the expansion coefficients A_{jm} ($j = 1, \dots, 4$) are as yet unknown. For summations in (13) and (14) over functions involving $\sin(m\phi)$, the index m extends over $\{1, \infty\}$; while for those involving $\cos(m\phi)$, the index m assumes values in the range $\{0, \infty\}$.

Pertinent to the present problem, however, the foregoing expressions hold rigorously only if $L > 8a/3$, but cannot be deemed to be valid rigorously if $L < 8a/3$. In the latter case, this method must be held *a priori* to be an approximate one. Should, however, the cylinders intersect, i.e., if $L < 2a$, then together they form an infinitely long material plate with periodically rough boundaries, and techniques like the ones described in Refs. 8 and 9 may be used to solve for the reflection and transmission problem.

THE COMPLETE SOLUTION

In the region $|y| \geq a$, the appropriate representation of both the elastic and the EM fields is in terms of the Bloch wave functions with periodicity L . Consequently, for $y \geq a$, $-\infty < x < \infty$,

$$u_{z+} = \sum_n \{S_{1n+} \exp[-i\beta_n^{SH} y] + R_{1n+} \exp[i\beta_n^{SH} y]\} \exp[i\alpha_n x] \quad (15)$$

$$H_{z+} = -i\omega \sum_n \{S_{2n+} \exp[-i\beta_n^H y] + R_{2n+} \exp[i\beta_n^H y]\} \exp[i\alpha_n x] \quad (16)$$

where,

$$\alpha_n = \alpha_0 + n(2\pi/L), \quad n = 0, \pm 1, \pm 2, \dots, \quad (17a)$$

$$\beta_n^{SH} = + \{k_{SH1}^2 - \alpha_n^2\}^{1/2}, \quad (17b)$$

$$\beta_n^H = + \{k_{H1}^2 - \alpha_n^2\}^{1/2}, \quad (17c)$$

and α_0 is a parameter decided by the PWS expansion of the incident field [7], and will be given later.

Likewise, for $y \leq -a$, $-\infty < x < \infty$, the fields can be set down as

$$u_{z-} = \sum_n \{S_{1n-} \exp[-i\beta_n^{SH} y] + R_{1n-} \exp[i\beta_n^{SH} y]\} \exp[i\alpha_n x] \quad (18)$$

$$H_{z-} = -i\omega \sum_n \{S_{2n-} \exp[-i\beta_n^H y] + R_{2n-} \exp[i\beta_n^H y]\} \exp[i\alpha_n x]. \quad (19)$$

In these field expressions, the planewave ensembles $\{S_{1n+}\}$, $\{S_{2n+}\}$, $\{R_{1n-}\}$ and $\{R_{2n-}\}$ represent plane waves *moving towards* the cylinder array, and could be propagating or evanescent. The remaining ensembles, $\{S_{1n-}\}$, $\{S_{2n-}\}$, $\{R_{1n+}\}$ and $\{R_{2n+}\}$ represent plane waves *moving away* from the array. Since only the reflection and transmission of a SH wave is going to be considered here, it follows that

$$S_{2n+} = R_{1n-} = R_{2n-} = 0, \quad \forall n; \quad S_{1n+} = \delta_{n0}, \quad (20a)$$

where δ_{nm} is the Kronecker delta; the remaining coefficients in (15), (16), (18) and (19) need to be determined. In addition, since the incident SH wave will be taken to be a plane wave making an angle ϑ_0^{SH} with the y axis,

$$\alpha_0 = k_{SH1} \sin(\vartheta_0^{SH}). \quad (20b)$$

It now remains to link the various coefficients A_{jm} ($j = 1, \dots, 4$) with the plane wave coefficients of this section in order to obtain the scattering characteristics of the piezoelectric cylinder array. It would be useful, however, to exploit the symmetries of the elastic and the EM fields about the y axis. Thus, let all of the fields to be decomposed as follows:

$$\zeta(x, y) = (1/2) [\zeta_e(x, y) + \zeta_o(x, y)], \quad (21a)$$

where

$$\zeta_e(x, y) = [\zeta(x, y) + \zeta(x, -y)], \quad (21b)$$

and

$$\zeta_o(x, y) = [\zeta(x, y) - \zeta(x, -y)]; \quad (21c)$$

and this decomposition is forced upon the expansions (13) - (16), (18) and (19).

On enforcing the continuity of the *even magnetic* and the *odd displacement* fields, as well as of their y-derivatives, across $y = a$, $|x| \leq L/2$ and eliminating the coefficients A_{3m} and A_{4m} leads to the matrix equation [10,11]:

$$\left(\begin{array}{c|c} U_1 & U_2 \\ \hline U_3 & U_4 \end{array} \right) \left(\begin{array}{c} S_{1+} + R_{1-} \\ \hline S_{1-} + R_{1+} \end{array} \right) = \left(\begin{array}{c} S_{2+} - R_{2-} \\ \hline R_{2+} - S_{2-} \end{array} \right), \quad (22a)$$

where

$$\begin{aligned} \left(\begin{array}{c|c} U_1 & U_2 \\ \hline U_3 & U_4 \end{array} \right) &= \left(\begin{array}{c|c} N_1^H & N_2^H \\ \hline N_3^H & N_4^H \end{array} \right)^{-1} \left(\begin{array}{c|c} M_1^H & M_2^H \\ \hline M_3^H & M_4^H \end{array} \right) \cdot \\ &\cdot \left(\begin{array}{c|c} M_1^{SH} & M_2^{SH} \\ \hline M_3^{SH} & M_4^{SH} \end{array} \right)^{-1} \left(\begin{array}{c|c} N_1^{SH} & N_2^{SH} \\ \hline N_3^{SH} & N_4^{SH} \end{array} \right), \end{aligned} \quad (22b)$$

and the various matrices of (22b) are given in the Appendix.

Similarly, on enforcing the continuity of the *odd magnetic* and the *even displacement* fields, as well as of their y-derivatives, across $y = a$, $|x| \leq L/2$ and eliminating the coefficients A_{1m} and A_{2m} leads to the matrix equation [10,11]:

$$\left(\begin{array}{c|c} V_1 & V_2 \\ \hline V_3 & V_4 \end{array} \right) \left(\begin{array}{c} S_{2+} + R_{2-} \\ \hline S_{2-} + R_{2+} \end{array} \right) = \left(\begin{array}{c} S_{1+} - R_{1-} \\ \hline R_{1+} - S_{1-} \end{array} \right), \quad (23a)$$

where

$$\begin{pmatrix} V_1 & V_2 \\ V_3 & V_4 \end{pmatrix} = \begin{pmatrix} N_1^{SH} & N_2^{SH} \\ N_3^{SH} & N_4^{SH} \end{pmatrix}^{-1} \begin{pmatrix} M_5^{SH} & M_6^{SH} \\ M_7^{SH} & M_8^{SH} \end{pmatrix} \cdot \begin{pmatrix} M_5^H & M_6^H \\ M_7^H & M_8^H \end{pmatrix}^{-1} \begin{pmatrix} N_1^H & N_2^H \\ N_3^H & N_4^H \end{pmatrix}, \quad (23b)$$

and the various matrices of (23b) are also given in the Appendix.

Rearrangement of (22a) and (23a) finally gives a system T-matrix for the periodic array

$$[S_{1-}; R_{1+}; S_{2-}; R_{2+}]^{Tr} = [T] [S_{1+}; R_{1-}; S_{1+}; R_{1-}]^{Tr} \quad (24a)$$

where Tr denotes transpose, and the matrix

$$[T] = - \begin{bmatrix} U_2 & | & U_2 & | & 0 & | & 0 \\ \hline U_4 & & U_4 & & I & & -I \\ \hline 0 & & 0 & & V_2 & | & V_2 \\ \hline I & & -I & & V_4 & | & V_4 \\ \hline U_1 & | & U_1 & | & -I & | & I \\ \hline U_3 & & U_3 & & 0 & & 0 \\ \hline -I & & I & & V_1 & & V_1 \\ \hline 0 & & 0 & & V_3 & & V_3 \end{bmatrix}^{-1} \cdot \quad (24b)$$

with I being the identity matrix.

Of necessity, all of the submatrices involved in (22) - (24) are truncated to be of size $(2N+1) \times (2N+1)$. Recalling (20a), the principle of conservation of energy can be used to determine the truncation parameter N . The requirement that the final solution preserve the unitarity relation

$$\begin{aligned} & \sum_n \text{Re}\{\beta_n^{SH}\} [|S_{1n-}|^2 + |R_{1n+}|^2] / \beta_0^{SH} \\ & + \sum_n (\mu_1/\epsilon_1)^{1/2} (\omega^2/\pi c_{441} \beta_0^{SH}) \text{Re}\{\beta_n^{H/k_{H1}}\} [|S_{2n-}|^2 + |R_{2n+}|^2] = 1 \end{aligned} \quad (25)$$

within an adequate error tolerance ($\pm 0.5\%$) determines its convergence. Additionally, the various coefficients $S_{pn\pm}$, $R_{pn\pm}$ ($p = 1, 2$) should also converge within an acceptable error bound, say not exceeding 1.0% , and this requirement can also be used to check the accuracy and the adequacy of the computed solution.

THE QUASI-STATIC APPROXIMATION

The solution procedure outlined above is indeed complete; however, because of the wide disparity between the wavenumbers k_{SH1} and k_{H1} , what are high-frequency elastic waves are found to be coupled with very low-frequency EM waves. Since the normalised distance $k_{H1}L \ll k_{SH1}L$, and because the energy conversion mechanism is not a very strong one (i.e., D_m and F_m are very small compared with the other coefficients C_m and E_m), it is possible to use a *quasi-static* approximation quite fruitfully.

In view of the incidence conditions (20a), the interaction of electromagnetic and elastic waves can be initially *ignored*. Thus,

$$\begin{pmatrix} Z_1 & Z_1 \\ Z_3 & -Z_3 \end{pmatrix} \begin{pmatrix} S_{1+} \\ R_{1-} \end{pmatrix} = \begin{pmatrix} Z_2 & Z_2 \\ -Z_4 & Z_4 \end{pmatrix} \begin{pmatrix} S_{1-} \\ R_{1+} \end{pmatrix} \quad (26)$$

can be derived from (22) and (23), where the submatrices

$$Z_1 = M_3^{SH} \cdot [M_1^{SH}]^{-1} \cdot N_1^{SH} - N_3^{SH} \quad (27a)$$

$$Z_1 = -M_3^{SH} \cdot [M_1^{SH}]^{-1} \cdot N_2^{SH} + N_4^{SH} \quad (27b)$$

$$Z_1 = M_7^{SH} \cdot [M_5^{SH}]^{-1} \cdot N_1^{SH} - N_3^{SH} \quad (27c)$$

$$Z_1 = -M_7^{SH} \cdot [M_5^{SH}]^{-1} \cdot N_2^{SH} + N_4^{SH} \quad (27d)$$

and

$$A_{2m} = 0, A_{4m} = 0, \quad \forall m \quad (28)$$

Once the SH coefficients S_{1n-} and R_{1n+} have been determined from (26), the coefficients A_{1m} and A_{3m} can be found from the matrix relations:

$$\{A_1\} = [M_1^{SH}]^{-1} \cdot N_1^{SH} \cdot \{S_{1+} + R_{1-}\} + [M_1^{SH}]^{-1} \cdot N_2^{SH} \cdot \{S_{1-} + R_{1+}\}, \quad (29a)$$

$$\{A_3\} = [M_5^{SH}]^{-1} \cdot N_1^{SH} \cdot \{S_{1+} - R_{1-}\} + [M_5^{SH}]^{-1} \cdot N_2^{SH} \cdot \{R_{1+} - S_{1-}\}. \quad (29b)$$

Substitution of (28) and (29) in (13) and (14) gives the elastic and the electromagnetic fields, u_z^{unit} and H_z^{unit} , respectively, in the unit cell outside the piezoelectric cylinder. Insofar as the fields generated inside the cylinder in each unit cell are concerned, they can be computed from the relations [5]:

$$u_z^{\text{int, unit}} = \sum_m A_{1m} G_m J_m(k_{SH2}r) \cos m\phi + i \sum_m A_{3m} G_m J_m(k_{SH2}r) \sin m\phi, \quad (30)$$

and

$$H_z^{\text{int, unit}} = -i\omega \left(\sum_m A_{3m} I_m J_m(k_{H2}r) \cos m\phi + \sum_m A_{1m} I_m J_m(k_{H2}r) \sin m\phi \right), \quad (31)$$

where

$$\Delta_m G_m = (-2ic_{441}/\pi) [(\epsilon_2/\epsilon_1)(k_{H1}a) H_m'(k_{H1}a) J_m(k_{H2}a) - (k_{H2}a) H_m(k_{H1}a) J_m'(k_{H2}a)], \quad (32)$$

and

$$\Delta_m I_m = (2me_{152}c_{441}/\pi)J_m(k_{SH2}a)H_m(k_{H1}a). \quad (33)$$

Furthermore, the voltage difference V_{12} between two points $\{a, \phi_1\}$ and $\{a, \phi_1 + \pi\}$ in a unit cell can be computed in the following manner:

$$V_{12} = - \int_0^a dr [E_r^{\text{int,unit}}(r, \phi_1) + E_r^{\text{int,unit}}(r, \phi_1 + \pi)] \quad (34)$$

where,

$$\epsilon_{T2} E_r^{\text{int,unit}} = [(1/r) \partial/\partial \phi \{iH_z^{\text{int,unit}}/\omega\} - e_{152} \partial/\partial r \{u_z^{\text{int,unit}}\}]; \quad (35)$$

whence,

$$V_{12} = (-2/\epsilon_{T2}) \sum_{m=0,2,4,\dots} A_{1m} \cos m \phi_1 \left[iI_m \left\{ 1 - (2/k_{H2}a) \sum_{k=1,\dots,m/2} [(2k-1)J_{2k-1}(k_{H2}a)] \right\} - e_{152} G_m \{ J_m(k_{SH2}a) - J_m(0) \} \right]. \quad (36)$$

NUMERICAL RESULTS AND DISCUSSION

The quasi-static approximation of the previous section was implemented on a DEC VAX 11/730 minicomputer for piezoelectric cylinders of radii $a = 0.2\text{cm}$ immersed in a homogeneous medium whose constitutive parameters are $\epsilon_1 = 7.0\epsilon_0$, $\mu_1 = \mu_0$, $\rho_1 = 1100 \text{ kg m}^{-3}$ and $c_{441} = 7.0 \times 10^7 \text{ N m}^{-2}$. The parameters for the cylinders themselves were taken to be $\epsilon_2 = 301.0\epsilon_0$, $\mu_2 = \mu_0$, $\rho_2 = 6600 \text{ kg m}^{-3}$ and $c_{442} = 8.5 \times 10^9 \text{ N m}^{-2}$, with the piezoelectric coupling constant for medium 2 to be $e_{152} = 11.6 \text{ C N}^{-1}$. It has been earlier [12] that in a composite medium consisting of a random array of such cylinders immersed in the selected medium 1 gives rise to increased attenuation of SH waves, in general. The end-result of these computations are the time-averaged Poynting vectors of the SH waves reflected (R_n) and transmitted (T_n) in medium 1 when a plane SH wave strikes the cylindrical array making an angle ϑ_0^{SH} with the y axis. The power diffraction coefficients are given as

$$R_n = |R_{1n+}|^2 \text{Re}\{\beta_n^{\text{SH}}\}/\beta_0^{\text{SH}} \quad (37)$$

and

$$T_n = |S_{1n-}|^2 \text{Re}\{\beta_n^{\text{SH}}\}/\beta_0^{\text{SH}}, \quad (38)$$

and are obviously non-zero so long as $|\alpha_n/k_{SH1}| \leq 1.0$. Additionally, calculations of the voltage V_{12} of (36) were also made with $\phi_1 = \pi/2$.

Plotted in Fig. 2 is R_0 for the case when $\vartheta_0^{\text{SH}} = 0^\circ$ and $L = 0.6\text{cm}$. This calculation was successfully performed upto a frequency of 42kHz, after which frequency convergence did not take place. This is due to the fact that the integrals of the submatrices involved (given in the Appendix) contain highly oscillatory integrands, and their computation, therefore, is prone to error. Although an efficient code [13] for computing the Bessel and Hankel functions was used here, still no confidence could be placed in the computed results beyond 42kHz frequency. In any case, $T_0 = 1.0 - R_0$ for the presented range of calculations, and no higher order transmitted or reflected modes carried any energy, i.e., $R_n = T_n = 0 \forall n \geq 1$. Also shown in Fig. 2 is the computed voltage V_{12} for $\phi_1 = \pi/2$.

In Fig. 3 the calculations were repeated but with the periodicity $L = 0.8\text{cm}$ for frequencies upto 49kHz. The plots of R_0 and T_0 show anomalous behaviour at about 31.5kHz. Such an anomaly is

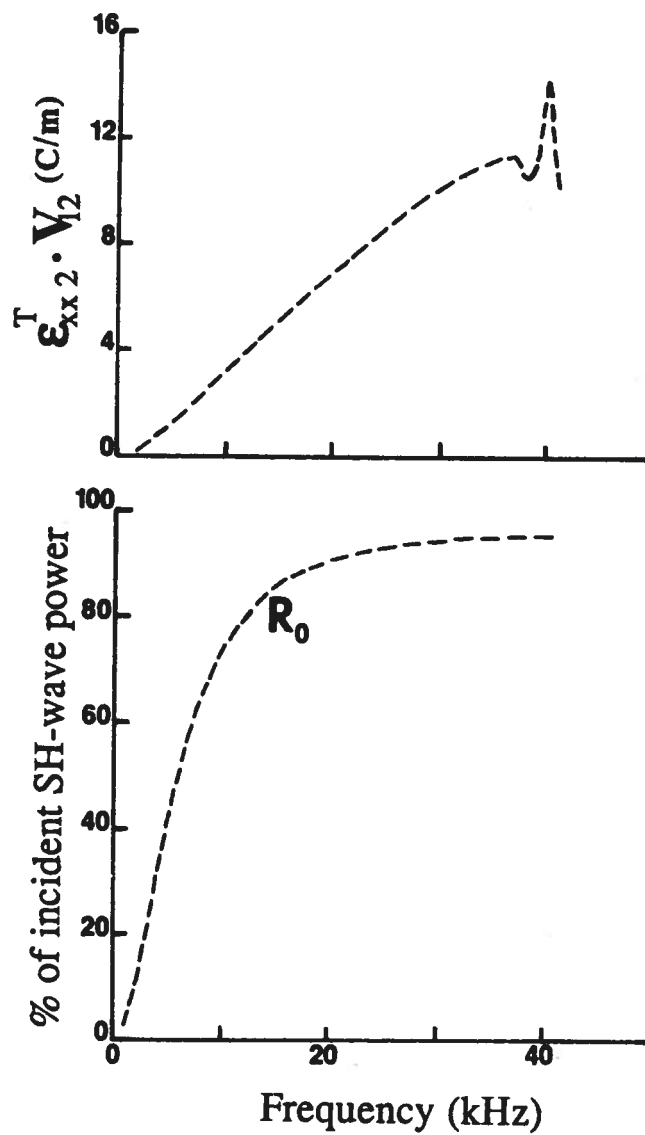


Figure 2. Specular reflection coefficient R_0 and the voltage V_{12} computed between points $\{a, \pi/2\}$ and $\{a, 3\pi/2\}$ when a plane SH wave hits the cylinder array ($L = 0.6\text{cm}$, $a = 0.2\text{cm}$) at an angle of $\vartheta_0^{\text{SH}} = 0^\circ$.

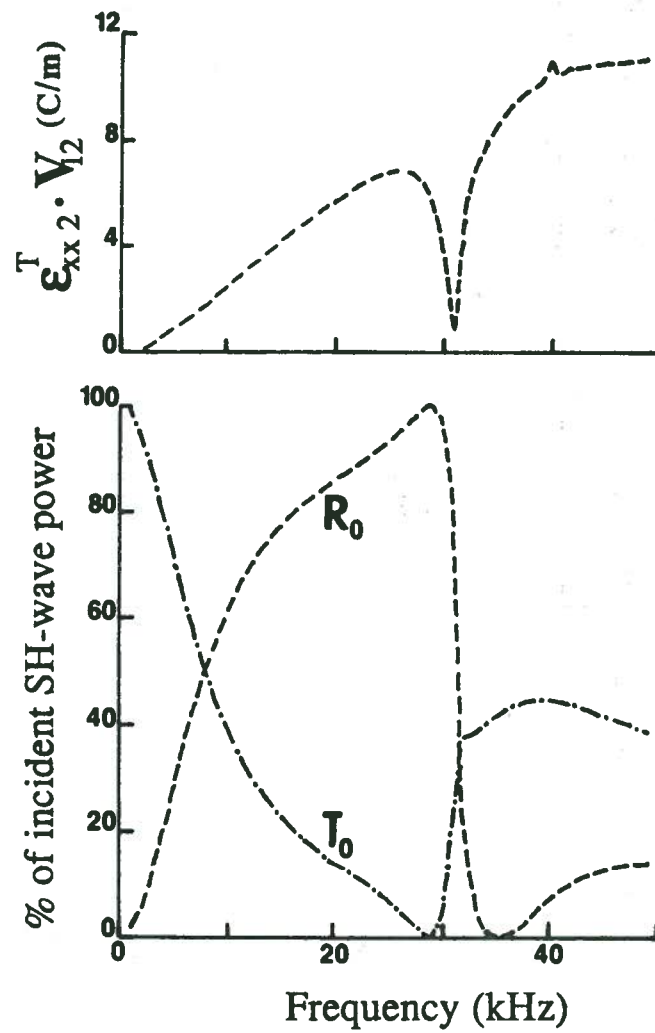


Figure 3. Specular reflection coefficient R_0 , specular transmission coefficient T_0 , and the voltage V_{12} computed between points $\{a, \pi/2\}$ and $\{a, 3\pi/4\}$ (pen 10 713 gm 0 0 728 567 6 direct %%Trailer end L = 0.8cm, $a = 0.2$ cm) at an angle of $\vartheta_0^{SH} = 0^\circ$.

called a Rayleigh-Wood anomaly [14], and comes here since the ± 1 th modes have been excited here, and, from this frequency onwards, propagate non-zero energies. However, $R_{\pm 1}$ and $T_{\pm 1}$ have not been plotted here for purposes of clarity. It is curious that, in spite of the use of the quasi-static approximation, the voltage V_{12} also records the Rayleigh-Wood anomaly as well as do R_0 and T_0 .

A similar comment regarding the ability of the computed voltage V_{12} to reflect the Rayleigh-Wood anomalies also holds in Figs. 4 - 6. In all of these three figures, $\theta_0^{SH} = 30^\circ$, but $L = 0.6\text{cm}$ (Fig.4), 0.8cm (Fig.5) and 1.0cm (Fig.6). Again, V_{12} reflects all of the Rayleigh-Wood anomalies which appear in the R_n - and the T_n - profiles.

A couple of general comments regarding the presented calculations are now in order. Firstly, it was found that by ignoring the piezoelectric coupling e_{152} , the total reflected power $\sum_n R_n$ was generally decremented by a small quantity, not exceeding 0.5% of the total incident power. As a compensation, the total transmitted power $\sum_n T_n$ would be incremented by the same amount when e_{152} was set equal to zero. Thus, at least for the present calculations and the frequencies considered, it can be safely stated that the piezoelectric properties of the cylinders did not greatly affect their elastic scattering characteristics.

Secondly, and perhaps more importantly, all of the V_{12} - profiles shown here contain an additional anomaly at frequencies around 40kHz. Although at first glance this looks surprising, this anomaly, whose location depends only on the cylinder shape, size and constitutive parameters, is similar to the impedance-frequency characteristic of the quartz-crystal oscillators [15]. Presumably, therefore, a transmission line model [5] of the piezoelectric cylinder will be able to predict this behavior. It is interesting, however, to observe this characteristic behavior of crystal oscillators in a scattering problem.

Lastly, the very high values of V_{12} need some clarification. From a computational standpoint, such high values result from the presence of the Hankel function $H_m(k_{H1}a)$ in the formula (33) for I_m . Since, $k_{H1}a$ is a very small quantity at these frequencies, the Hankel function becomes extremely large, thereby making I_m also very large. Consequently, the EM field excited inside each cylinder is very high, although it does not radiate outwards enough to merit any effect on the satisfaction of the principle of conservation of energy. Therefore, V_{12} is also very large. However, it is to be noted that it is an open-circuit voltage. Presumably, when a pair of leads is put across the cylinder in order to tap this high voltage, it will immediately drop to very low values and will need amplification in order to be measured.

ACKNOWLEDGEMENT

The assistance of Dr. Yushieh Ma of the Pennsylvania State University is greatly appreciated in many discussions regarding the subject of this communication.

APPENDIX

The matrix elements of (22b) and (23b) are as follows:

$$\{N_1^P\}_{nm} = \delta_{nm} \exp[-i\beta_n^P \cdot a] ; \quad p = SH, H \quad (A1)$$

$$\{N_2^P\}_{nm} = \delta_{nm} \exp[i\beta_n^P \cdot a] ; \quad p = SH, H \quad (A2)$$

$$\{N_3^P\}_{nm} = -i\beta_n^P \{N_1^P\}_{nm} ; \quad p = SH, H \quad (A3)$$

$$\{N_4^P\}_{nm} = i\beta_n^P \{N_2^P\}_{nm} ; \quad p = SH, H \quad (A4)$$

$$\{M_1^{SH}\}_{nm} = \int dx \exp[-i\alpha_n x] \{\cos m\phi\} [J_m(k_{SH1}r) + C_m H_m(k_{SH1}r)] \Big|_{y=a} \quad (A5)$$

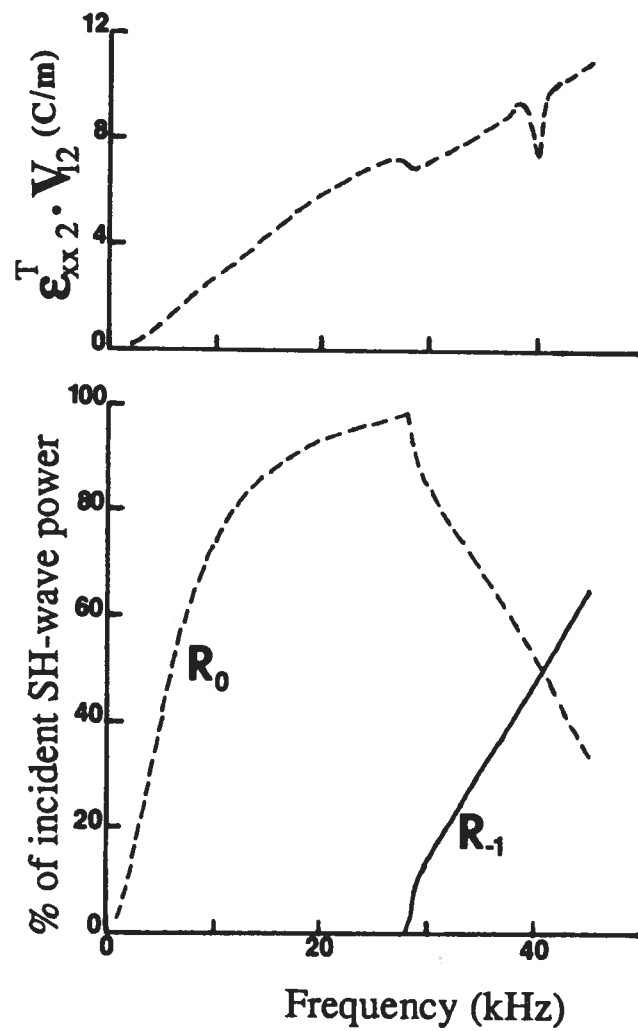


Figure 4. Reflection coefficients R_0 and R_{-1} , and the voltage V_{12} computed between points $\{a, \pi/2\}$ and $\{a, 3\pi/2\}$ when a plane SH wave hits the cylinder array ($L = 0.6\text{cm}$, $a = 0.2\text{cm}$) at an angle of $\vartheta_0^{\text{SH}} = 30^\circ$.

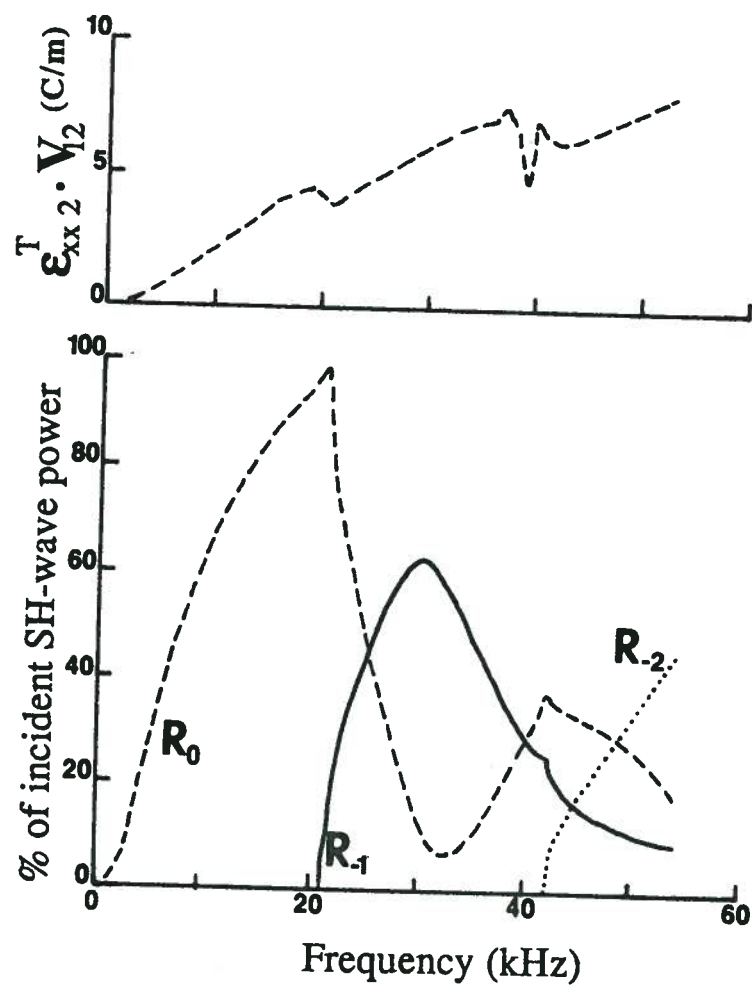


Figure 5. Reflection coefficients R_0 , R_1 and R_2 and the voltage V_{12} computed between points $\{a, \pi/2\}$ and $\{a, 3\pi/2\}$ when a plane SH wave hits the cylinder array ($L = 0.8\text{cm}$, $a = 0.2\text{cm}$) at an angle of $\vartheta_0^{\text{SH}} = 30^\circ$.

10. Lakhtakia, A., V.V. Varadan and V.K. Varadan, 'Reflection characteristics of an elastic slab containing a periodic array of elastic cylinders: SH wave analysis,' *J. Acoust. Soc. Am.*, submitted for publication (1985).
11. Lakhtakia, A., V.V. Varadan and V.K. Varadan, 'Reflection characteristics of a dielectric slab containing dielectric or perfectly conducting cylindrical gratings,' *Appl. Opt.*, to appear (1986).
12. Varadan, V.K., V.V. Varadan and Y. Ma, *Multiple scattering of elastic waves by piezo-electric cylinders in rubber-like materials. I*, Rept. No. PSU/LEAR-85-3, Department of Engineering Science and Mechanics, The Pennsylvania State University (1985).
13. Mason, J.P., *Cylindrical Bessel functions for a large range of complex arguments*, Rept. No. NRL 8687, Naval Research Laboratory, Washington D.C. (1983).
14. Jordan, A.K. and R.H. Lang, 'Electromagnetic scattering patterns from sinusoidal surfaces,' *Rad. Sci.*, 14, 1077-1088 (1981).
15. Fink, D.G. and A.A. McKenzie (Eds.), *Electronics Engineer's Handbook*, Sec. 13-38, McGraw-Hill, New York (1975).